Anisotropic renormalization of thermodynamic quantities above the nematic–smectic-A phase transition

Barbara S. Andereck
Department of Physics and Astronomy, Ohio Wesleyan University, Delaware, Ohio 43015
and Department of Physics, The Ohio State University, Columbus, Ohio 43210

Bruce R. Patton
Department of Physics, The Ohio State University, Columbus, Ohio 43210
(Received 14 July 1993)

The results of a self-consistent, one-loop model for the nematic–smectic-A phase transition are presented. Fluctuation-induced renormalization of the correlation lengths parallel and perpendicular to the director and of the twist and bend elastic constants are calculated. The inherently anisotropic nature of the coupling between the director fluctuations and the smectic order parameter directly leads to anisotropic renormalization of the correlation lengths and elastic constants. Because the renormalization of the four quantities mentioned above becomes significant at different temperatures, the crossover from the isotropic high-temperature behavior to the critical, strongly anisotropic behavior is very gradual, producing an extended, weakly anisotropic region, consistent with experimental observations.

PACS number(s): 64.70.Md

I. INTRODUCTION

One of the most interesting and complicated phase transitions in nature occurs between the nematic (N) and smectic-A (A) phases in liquid-crystal systems. The nature of the critical behavior above the N-A transition has been studied experimentally [1] and theoretically [2–6] for 20 years, with unsatisfactory agreement, not only between theory and experiment, but from one experimental study to another. The free energy proposed by de Gennes [7,8] has formed the basis of the theories, but even with this same starting point different approaches have predicted different universality classes for the transition. The most puzzling unexplained experimental behavior had been the universal weak anisotropy of critical exponents that spanned three or more decades in reduced temperature. Recently we outlined a straightforward calculation based on de Gennes' free energy that predicts a gradual crossover from isotropic to anisotropic critical behavior and also a broad, weakly anisotropic region of the type seen experimentally [9]. In this paper we present the details of our calculations and results. In Sec. II we describe the liquid-crystal phases and introduce the form of the free energy used. In Sec. III we discuss the formal theory for the correlation functions describing the fluctuations of the smectic order parameter and the nematic director. In Sec. IV we present the self-consistent one-loop model that we use to simplify the calculation of the correlation functions. The properties of these correlation functions (that ultimately lead to anisotropic critical behavior) are crucially dependent on the anisotropic interaction of the smectic order parameter and the fluctuations in the director. This one-loop model is used in Sec. V to calculate the spatially uniform ($\mathbf{k}=\mathbf{0}$) limit of the self-energies and the region where strong renormalization of the temperature scale is expected; this is found to be well below the temperatures reached by experiments to date, indicating that the coupling between the smectic order parameter and the director fluctuations does not affect the critical exponent γ in this range. Section VI extends the calculation of the correlation functions to the spatially inhomogeneous ($\mathbf{k}\neq\mathbf{0}$) case and determines the critical exponents $\nu_{\parallel}$ and $\nu_{\perp}$ associated with the parallel and perpendicular correlation lengths. In Sec. VII, using numerical solutions of the renormalization equations for the correlation lengths and the twist and bend elastic constants, we discuss anisotropies that develop in various temperature regimes as well as the asymptotic behavior of thermodynamic quantities close to the N-A transition. Plots of the solutions of the coupled equations are presented for a variety of parameters in the theory. The results indicate the onset of a weakly anisotropic region at a reduced temperature where the renormalization of the bend elastic constant becomes significant. In this weakly anisotropic region we find that $\nu_{\parallel}/\gamma$ remains unchanged at its high-temperature value of $\frac{1}{2}$, while $\nu_{\perp}/\gamma$ decreases from the high-temperature value of $\frac{1}{2}$ and approaches $\frac{3}{8}$. At a lower reduced temperature, where the smectic-director coupling begins to affect γ, a strongly anisotropic region develops in which $\nu_{\parallel}/\gamma=1$ and $\nu_{\perp}/\gamma=\frac{1}{2}$. The critical exponents $\eta_{\parallel}$ and $\eta_{\perp}$ describing the behavior of the correlation function at the transition temperature are calculated as a check of the self-consistency of the model in Sec. VIII, and are found to satisfy the scaling laws $\nu_{\parallel}=\gamma/(2-\eta_{\parallel})$ and $\nu_{\perp}=\gamma/(2-\eta_{\perp})$. Section IX contains a summary of the results of the paper and some possible directions for future work.

II. STANDARD MODEL AND FREE ENERGY

The nematic phase of liquid crystals is characterized by orientational ordering of elongated liquid-crystal molecules about a common direction designated by a unit vec-

tor $\mathbf{n}$, the director. The centers of mass of the molecules are disordered in the nematic phase. The presence of the orientational order allows for splay, twist, and bend elastic restoring forces. The energy associated with these elastic deformations, proposed by Frank [6,10], can be written in the form

$$\mathcal{F}_{\rm el}=\frac{1}{2}\int\frac{d^3k}{(2\pi)^3}[(K_{10}k_\perp^2+K_{30}k_\parallel^2)\delta n_s^2 + (K_{20}k_\perp^2+K_{30}k_\parallel^2)\delta n_t^2]\ , \tag{1}$$

where K_{10}, K_{20}, and K_{30} are the bare splay, twist, and bend elastic constants, $\mathbf{k}_\perp$ and $k_\parallel$ are the components of the wave vector perpendicular and parallel to $\mathbf{n}$, and δn_s and δn_t are the splay and twist fluctuations of the director perpendicular to $\mathbf{n}_0$, parallel and perpendicular to $\mathbf{k}_\perp$, respectively.

Smectic liquid-crystal phases are characterized by the presence of a one-dimensional density wave. The order parameter $\psi(\mathbf{r})=f(\mathbf{r})\exp[i(\mathbf{q}_0\cdot\mathbf{r}+\phi)]$ for the smectic phases is a measure of the strength of the density wave [11],

$$\rho(\mathbf{r})=\rho_0(\mathbf{r})[1+f(\mathbf{r})\sin(\mathbf{q}_0\cdot\mathbf{r}-\phi)]\ , \tag{2}$$

where ρ is the density and $\mathbf{q}_0$ is the wave vector of the density wave. The Landau-Ginzburg free energy for the order parameter ψ, near the N-A transition, proposed originally by de Gennes [7,8] is

$$\beta\mathcal{F}_\psi=\int d^3r[t|\psi|^2+\frac{1}{2}b|\psi|^4 + (\nabla+iq_0\mathbf{n})_i\psi^*\Gamma_{ij}(\nabla-iq_0\mathbf{n})_j\psi]\ , \tag{3}$$

where β is the inverse temperature, $t=(T-T_c)/T_c$, b is constant, and

$$\Gamma=\begin{pmatrix}\xi_{10}^2 & 0 & 0\\ 0 & \xi_{10}^2 & 0\\ 0 & 0 & \xi_{\parallel 0}^2\end{pmatrix}\ , \tag{4}$$

where $\xi_{\perp 0}$ and $\xi_{\parallel 0}$ are the bare smectic correlation lengths perpendicular and parallel to $\mathbf{q}_0$. As required by global rotational invariance, the gradient term in Eq. (3) contains an explicitly anisotropic coupling between the director and the smectic order parameter; this interaction causes the director fluctuations to produce qualitatively different renormalizations of $\xi_\perp$ and $\xi_\parallel$, and also causes the smectic fluctuations, in turn, to produce a renormalization of the elastic constants [7,12] as the N-A transition is approached. A similar model, generalized to include smectic-C director fluctuations, has been used by the authors to describe the nematic–smectic-C transition [13].

III. FORMAL THEORY OF THE CORRELATION FUNCTIONS

The critical behavior near the N-A transition can be found by studying the smectic- and director-correlation functions $G(\mathbf{k})$ and $D_{s,t}(\mathbf{q})$, respectively:

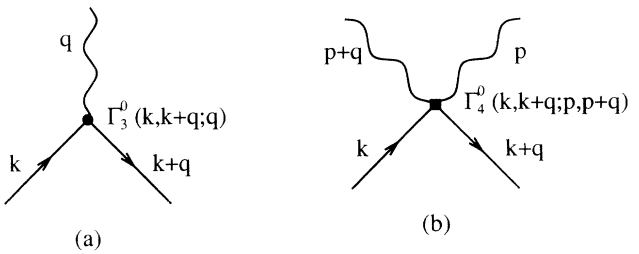

FIG. 1. Bare three- (a) and four-point (b) vertices arising from the gradient term coupling in the ψ-free energy in Eq. (3). Straight lines represent smectic correlation functions G, and wavy lines represent director correlation functions D.

$$G(\mathbf{k})=\langle\psi^*(\mathbf{k})\psi(\mathbf{k})\rangle=[G_0^{-1}(\mathbf{k})-\Sigma(\mathbf{k})]^{-1}\ , \tag{5a}$$

$$D_{s,t}(\mathbf{q})=\langle\delta n_{s,t}(\mathbf{q})\delta n_{s,t}(-\mathbf{q})\rangle =[D_{0s,t}^{-1}(\mathbf{q})-\Pi(\mathbf{q})]^{-1}\ , \tag{5b}$$

where the bare correlation functions are

$$G_0(\mathbf{k})=[t+\xi_{10}^2k_\perp^2+\xi_{\parallel 0}^2k_\parallel^2]^{-1}\ , \tag{6a}$$

$$D_{0s,t}(\mathbf{q})=\beta^{-1}[K_{1,2}^0q_\perp^2+K_3^0q_\parallel^2]^{-1}\ . \tag{6b}$$

We have used Dyson's equations to express the correlation functions $G(\mathbf{k})$ and $D(\mathbf{q})$ in terms of the self-energy functions $\Sigma(\mathbf{k})$ and $\Pi(\mathbf{q})$ which arise from the interaction between the bare smectic and nematic modes G_0 and $D_{0s,t}$. Inspection of Eq. (3) reveals that the interactions arise from the gradient term, which contains both three- and four-point vertices connecting $\delta\mathbf{n}$ and ψ, as illustrated in Fig. 1. The bare three-point vertices, connecting $G_0(\mathbf{k})$, $G_0(\mathbf{k}+\mathbf{q})$, and $D_{0s,t}(\mathbf{q})$, have the momentum-dependent form

$$\Gamma_{3s}^0(\mathbf{k},\mathbf{k}+\mathbf{q};\mathbf{q})=-q_0\xi_{10}^2\hat{\mathbf{q}}_\perp\cdot(2\mathbf{k}_\perp+\mathbf{q}_\perp) \equiv-q_0\xi_{10}^2(2k_{\perp s}+q_\perp)\ , \tag{7a}$$

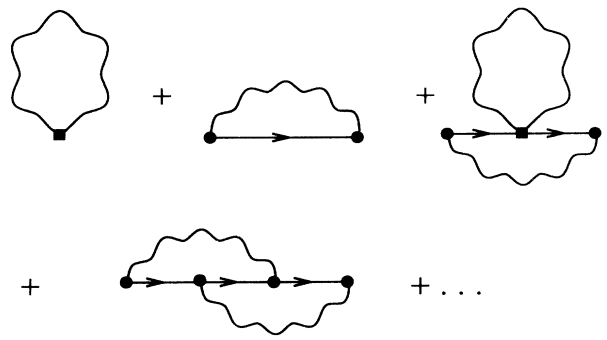

FIG. 2. Representative terms in the expansion of the smectic self-energy Σ in terms of bare correlation functions and vertices.

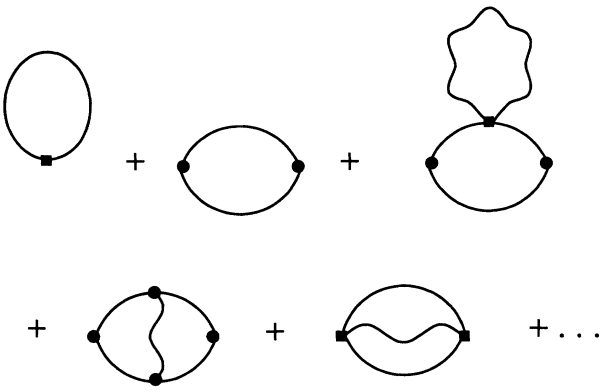

FIG. 3. Representative terms in the expansion of the director self-energy Π in terms of bare correlation functions and vertices.

$$\Gamma^0_{3t}(\mathbf{k},\mathbf{k}+\mathbf{q};\mathbf{q}) = -q_0\xi^2_{10}\hat{\mathbf{n}}_0\cdot[\hat{\mathbf{q}}_\perp\times(2\mathbf{k}_\perp+\mathbf{q}_\perp)]$$

$$\equiv -q_0\xi^2_{10}(2k_{\perp t}) \,, \tag{7b}$$

where s and t stand for splay and twist and $k_{\perp s}(k_{\perp t})$ is the component of $\mathbf{k}_\perp$ along (perpendicular to) $\mathbf{q}_\perp$. The bare four-point vertex, connecting $G_0(\mathbf{k})$, $G_0(\mathbf{k}+\mathbf{q})$, $D_{0s,t}(\mathbf{p})$, and $D_{0s,t}(\mathbf{p}+\mathbf{q})$ is momentum independent:

$$\Gamma^0_4(\mathbf{k},\mathbf{k}+\mathbf{q};\mathbf{p},\mathbf{p}+\mathbf{q}) = q_0^2\xi^2_{10} \,. \tag{8}$$

The self-energies $\Sigma(\mathbf{k})$ and $\Pi(\mathbf{q})$ are given by an expansion in terms of the bare interactions $\Gamma^0_{3s,t}$ and Γ^0_4 together with the bare propagators $G_0(\mathbf{k})$ and $D_{0s,t}(\mathbf{q})$, as shown in Figs. 2 and 3, respectively. Examination of this expansion reveals that the terms may be resummed into renormalized skeleton graphs in the usual way as shown in Figs. 4 and 5 by introducing renormalized propagators as well as renormalized vertices $\Gamma_{3s,t}$ and Γ_4 [14]. Note that in order to avoid double counting, the Γ^0_4 vertex in the Hartree diagram and the first $\Gamma^0_{3s,t}$ vertex in the second diagram are not renormalized in both cases. The dressed interactions $\Gamma_{3s,t}$ and Γ_4 are themselves given by an expansion in terms of dressed interactions and propagators as shown in Fig. 6. In Sec. IV we consider a model in which these self-consistent expansions for $D(\mathbf{q})$ and $G(\mathbf{k})$ may be evaluated.

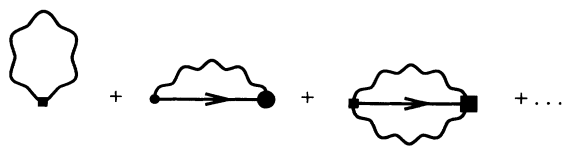

FIG. 4. Leading terms in the expansion of the smectic self-energy Σ in terms of renormalized correlation functions and bare and renormalized vertices. The first two terms are the only graphs kept in the one-loop model.

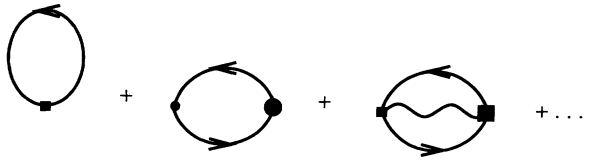

FIG. 5. Leading terms in the expansion of the director self-energy Π in terms of renormalized correlation functions and bare and renormalized vertices. The first two terms are the only graphs kept in the one-loop model.

IV. SELF-CONSISTENT, ONE-LOOP THEORY

We now consider the type of approximation we use to solve the set of coupled equations given above. We start with contributions from the large-N limit of the N-component theory, where N is the number of degrees of freedom of the ψ order parameter; this amounts to taking the leading one-loop contributions in the perturbation expansions for the self-energies in Figs. 4 and 5. It is known that this approximation gives a nontrivial description of a phase transition, including nonclassical (non-mean-field) exponents [15]. Next we impose the requirement that this approximation be a conserving one, so that conservation laws are preserved [16]. This last condition means that the propagators appearing in the one-loop contributions must be fully dressed, and that the dressed vertices must be determined self-consistently from the self-energies. Thus, although this approach starts by keeping terms of order $1/N$, it also keeps terms of higher order to satisfy self-consistency and thus preserve global rotational invariance and ensure that the elastic mode energies of the director vanish in the long-wavelength limit [i.e., that $D(\mathbf{q})$ remain massless] [7]. Thus, despite its similarities, the one-loop model represents a different approximation than the straightforward $1/N$ expansion [5].

In further justification of this approach we note that in the treatment of the one-loop model of massless scalar electrodynamics by Coleman and Weinberg [17], it was shown that this approximation gave a better treatment of the global minima of the system by treating all terms in the free energy on equal footing. Thus we may expect the one-loop approximation to give us the most unbiased

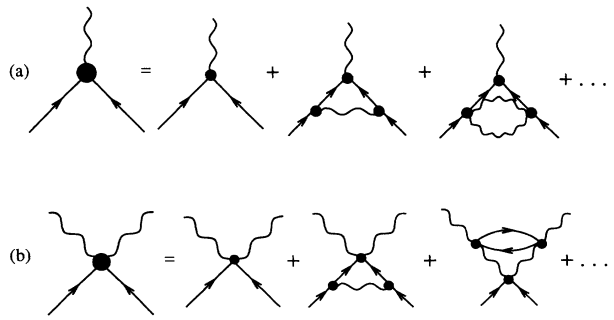

FIG. 6. Representative terms in the expansions of the three-(a) and four-point (b) renormalized vertices.

consideration of possible correlations leading to the phase transition. As Coleman and Weinberg show, the presence of two coupled fields (scalar meson and photon in their case, smectic order parameter and director fluctuation for our model) leads to a valid one-loop expansion for small coupling constants, which yields a correct description of the nontrivial minima in the free energy. This is not true for the expansion in an uncoupled system.

For the smectic fluctuation self-energy Σ, the first two terms in Fig. 4 contribute in the one-loop approximation:

$$\Sigma_{s,t}(\mathbf{k})=\int_{\mathbf{q}}\Gamma^0_{3s,3t}(\mathbf{k},\mathbf{k}+\mathbf{q};\mathbf{q})D_{s,t}(\mathbf{q}) \times G(\mathbf{k}+\mathbf{q})\Gamma_{3s,3t}(\mathbf{k}+\mathbf{q},\mathbf{k};-\mathbf{q}) - \int_{\mathbf{q}}\Gamma^0_4 D_{s,t}(\mathbf{q}) \ . \tag{9}$$

For the director-fluctuation self-energy we have, from Fig. 5, to the same order

$$\Pi_{s,t}(\mathbf{q})=\int_{\mathbf{k}}\Gamma^0_{3s,3t}(\mathbf{k},\mathbf{k}+\mathbf{q};\mathbf{q})G(\mathbf{k}) \times G(\mathbf{k}+\mathbf{q})\Gamma_{3s,3t}(\mathbf{k}+\mathbf{q},\mathbf{k};-\mathbf{q}) - \int_{\mathbf{k}}\Gamma^0_4 G(\mathbf{k}) \ . \tag{10}$$

These equations are nonlinear, self-consistent expressions determining the self-energies $\Sigma(\mathbf{k})$ and Π, since both the dressed propagators G and D, as well as the dressed vertices $\Gamma_{3s,t}$ depend on Σ and Π. We will evaluate these expressions by determining effective expressions for G, D, and $\Gamma_{3s,t}$ which permit carrying out the integrals.

It is possible to relate the renormalized vertices $\Gamma_{3s,t}$ to the self-energy Σ from a Ward identity which arises from the global rotational invariance of the theory. We derive the connection between these renormalized vertices and the renormalized perpendicular correlation length from the requirement that the mass of the director fluctuations must vanish above the transition. Consider the leading contributions to the director self-energy Π, as shown in Fig. 5. If the director mode is to remain hydrodynamic as the transition is approached, then $\Pi(\mathbf{q}=0)$ must vanish. Formally, we must have

$$\Pi_{s,t}(\mathbf{q}=0)=0=-2\int_k\Gamma^0_4 G(\mathbf{k}) + \int_k\Gamma^0_{3s,t}(\mathbf{k},\mathbf{k};0)G^2(\mathbf{k})\,\Gamma_{3s,t}(\mathbf{k},\mathbf{k};0) \ . \tag{11}$$

But a simple mathematical identity is obtained by integrating by parts:

$$-2\int_k\Gamma^0_4 G(\mathbf{k})=-2\int_k q_0^2\xi_{10}^2\left[-k_{\perp s,t}\frac{\partial G(\mathbf{k})}{\partial k_{\perp s,t}}\right] =\int_k 2q_0^2\xi_{10}^2 k_{\perp s,t}\left[G^2\frac{\partial G^{-1}(\mathbf{k})}{\partial k_{\perp s,t}}\right] \ . \tag{12}$$

Thus, using Eqs. (11) and (12) with expressions (7), we find a relation between the splay and twist vertices Γ_{3s} and Γ_{3t} and the Green's function

$$\Gamma_{3s,t}(\hat{\mathbf{k}},0)=-q_0\frac{\partial G^{-1}(\mathbf{k})}{\partial k_{\perp s,t}}=\Gamma^0_{3s,t}(\hat{\mathbf{k}},0)-q_0\frac{\partial\Sigma(\mathbf{k})}{\partial k_{\perp s,t}} \ . \tag{13}$$

V. EVALUATION OF THE ONE-LOOP THEORY FOR $k=0$.

Close to the phase transition where long wavelengths dominate the problem, we may use the small-$\mathbf{k}$ limit of the correlation functions G and D. G must have the form

$$G^{-1}(\mathbf{k})=G_0^{-1}(\mathbf{k})-\Sigma(\mathbf{k}) =a[1+\xi_\perp^2k_\perp^2+\xi_\parallel^2(k_\parallel-q_0)^2+c\xi_\perp^4k_\perp^4] \ , \tag{14}$$

which defines the physical perpendicular and parallel correlation lengths $\xi_\perp$ and $\xi_\parallel$. The parameter c measures the non-Lorentzian character of the density-fluctuation spectrum and $a=G^{-1}(\mathbf{k}=0)$. Similarly we have

$$D_{s,t}^{-1}(\mathbf{q})=D_{0s,t}^{-1}(\mathbf{q})-\Pi_{s,t}(\mathbf{q})=\beta[K_{1,2}q_\perp^2+K_3q_\parallel^2] \ , \tag{15}$$

which defines the physical elastic constants K_1, K_2, and K_3.

We may now derive the forms for $\Gamma_{3s,t}$ required by the Ward identity arising from rotational invariance, by substituting the form of G from Eq. (14) into Eq. (13), which yields

$$\Gamma_{3s,t}(\mathbf{k},\mathbf{k}+\mathbf{q};\mathbf{q})|_{\mathbf{q}\to 0}=-2q_0a\xi_\perp^2k_{\perp s,t} \tag{16}$$

or, therefore,

$$\frac{\Gamma^0_{3s}}{\Gamma_{3s}}\equiv\frac{\xi^2_{\perp xy}}{\xi^2_\perp} \ . \tag{17}$$

Thus we find

$$\Gamma_{3s}(\mathbf{k},\mathbf{k}+\mathbf{q};\mathbf{q})=-q_0a\xi_\perp^2\hat{\mathbf{q}}_\perp\cdot(2\mathbf{k}+\mathbf{q}) \ , \tag{18}$$

where

$$\xi_{\perp,\parallel xy}\equiv\frac{\xi_{\perp,\parallel 0}}{\sqrt{a}} \ . \tag{19}$$

$\xi_{\perp,\parallel xy}$ are the temperature-dependent correlation lengths of the liquid-crystal system in the absence of the coupling between smectic and director fluctuations.

With these results we are now in a position to calculate the expressions for the self-energies given in Eqs. (9) and (10). The renormalization of the transition temperature and the exponent γ are determined by the $\mathbf{k}=\mathbf{0}$ value of $\Sigma(\mathbf{k})$, while the renormalization of the correlation lengths (and the exponents $\nu_\perp$, $\nu_\parallel$, $\eta_\perp$, and $\eta_\parallel$) arise from the $\mathbf{k}$ dependence of $\Sigma(\mathbf{k})$. The $\mathbf{q}=\mathbf{0}$ value of $\Pi(\mathbf{q})$ is guaranteed to vanish from the Ward identity above, while its finite $\mathbf{q}$ dependence determines the renormalization of the elastic constants.

In the remainder of this section we consider the temperature renormalization [$\Sigma(\mathbf{k}=0)$] effect and show that director-fluctuation effects are unimportant down to the lowest temperatures of interest. The exponent γ is defined by the relation

$$a=t-\Sigma(\mathbf{k}=\mathbf{0})\propto t^\gamma \ . \tag{20}$$

The form of the self-energy in the $\mathbf{k}\rightarrow\mathbf{0}$ limit is

$$\Sigma_{s,t}(0)=\int_{\mathbf{q}}\Gamma^{0}_{3s,3t}(0,-\mathbf{q};\mathbf{q})D_{s,t}(\mathbf{q}) \times G(\mathbf{q})\Gamma_{3s,3t}(\mathbf{q},0;-\mathbf{q})-\int_{\mathbf{q}}\Gamma^{0}_{4}D_{s,t}(\mathbf{q}) . \tag{21}$$

Using Eq. (7b) in Eq. (21), we find that as $\mathbf{k}\rightarrow\mathbf{0}$ the first term in the twist contribution to the self-energy vanishes. Thus the renormalization of T_c and the exponent γ are determined only by the splay term and the Hartree terms in Eq. (21). Substituting the expressions for the Green's functions Eqs. (14) and (15), as well as for the vertices [Eqs. (7), (8), and (16)], we obtain the result for $\Sigma(0)$:

$$\Sigma(0)=\frac{1}{\beta}\int_{q}(-q_0\xi_{10}^2q_\perp)[1+\xi_1^2q_\perp^2+\xi_\parallel^2(q_\parallel-q_0)^2]^{-1} \times[K_1q_\perp^2+K_3q_\parallel^2]^{-1}(-q_0\xi_1^2q_\perp) -\frac{1}{\beta}\int_{q}q_0^2\xi_{10}^2([K_1q_\perp^2+K_3q_\parallel^2]^{-1} +[K_2q_\perp^2+K_3q_\parallel^2]^{-1}) . \tag{22}$$

Evaluating the integrals gives an expression that depends on the temperature through the correlation lengths and elastic constants. Using the bare elastic constants and high-temperature (unrenormalized) expressions for the correlation lengths [Eq. (19)] allows us to estimate the point at which director fluctuations become important in determining the exponent γ; this result has the form of a large temperature-independent term plus a temperature-dependent term:

$$a=t-\Sigma(0)=t+a_\gamma^{1/2}(2/\pi+a^{1/2})=t'+a_\gamma^{1/2}a^{1/2} , \tag{23}$$

where t' is the shifted temperature which vanishes at $t=-2a_\gamma^{1/2}/\pi$, and a_γ, the temperature at which corrections to linear behavior of a appear, is

$$a_\gamma\approx\left[\frac{q_0^2\xi_{10}^2}{24\pi\beta K\xi_{\parallel 0}}\right]^2 , \tag{24}$$

where K is a typical bare elastic constant. The form of this result indicates that (a) the transition temperature is renormalized downward by the director fluctuations due to the constant term, and that (b) since the temperature-dependent term is negligible for $a>a_\gamma$, the value of γ is unchanged down to a characteristic temperature $a\approx a_\gamma$. In other words, a_γ is the effective Ginzburg criterion for the effect of the director fluctuations on renormalizing the critical exponent γ, and for typical liquid-crystal parameters a_γ is of order 10^{-8}.

On both theoretical and experimental grounds the value of a_γ is expected to be much less than the Ginzburg criterion a_G for the smectic-smectic interaction arising from the $|\psi|^4$ term in the free energy. Although a_G is very small in superconductors, the shorter correlation lengths in a liquid crystal should imply $a_G\approx 10^0-10^{-2}$ [3]. From an experimental point of view, if a_G were as small as a_γ, then γ would have the mean-field value $\gamma_{\rm mf}=1$ throughout the measured experimental range, in contradiction to what is observed ($\gamma\neq 1$).

Thus in the present experiments, it appears that the entire isotropic and weakly anisotropic region occurs *above* the temperature at which renormalization of γ due to director fluctuations occurs. If this is the case, the behavior of γ is determined by the $|\psi|^4$ term and is that of the three-dimensional (3D) xy model.

VI. EVALUATION OF THE ONE-LOOP THEORY FOR FINITE k

We now turn to the evaluation of the finite-k contributions to the self-energies, which lead to renormalization of the correlation lengths (from Σ) and elastic constants (from Π). The self-energy may be expanded in powers of k; for finite values of reduced temperature a, the expansion is analytic in k^2. We consider later the k dependence for $a=0$, which determines the critical exponent η.

In determining the finite k dependence of the self-energy, it is important to note that contributions come not only from the k dependence of the propagators in Eq. (9), but also from the momentum dependence of the vertices. In order to extract the leading k dependence, the diagrams in Figs. 4 and 5 are expanded in terms of bare correlation functions and vertices. A typical term in this expansion is shown in Fig. 7. The smectic density-wave fluctuation (straight line) on the bottom of the diagram carries the external momentum through the graph; a contribution to the k dependence arises from each bare propagator or Γ_3 vertex on the bottom line. The result of summing all these contributions is shown in Fig. 8, where it may be seen that the effect is to generate a dressed vertex on both sides of the diagram. The phenomenon is well known, for example, in transport theory, where one is interested in the leading frequency dependence of the conductivity.

Substituting for the vertices and noting the Hartree terms are momentum independent, the leading k dependence may be obtained from expanding equations of the form

$$\Sigma_s(\mathbf{k})=\int\frac{d^3q}{(2\pi)^3}(-q_0a\xi_1^2)^2[\hat{\mathbf{q}}_\perp\cdot(2\mathbf{k}_\perp+\mathbf{q}_\perp)]^2 \times D_s(\mathbf{q})G(\mathbf{k}+\mathbf{q}) , \tag{25a}$$

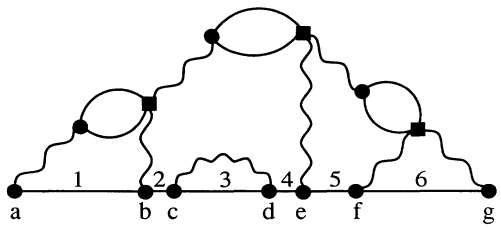

FIG. 7. Typical term in the expansion of the smectic self-energy. Expansion of Σ in terms of the external momentum is accomplished by extracting the leading momentum dependences from the bare smectic propagators designated by numbers, and the bare three-point vertices designated by letters.

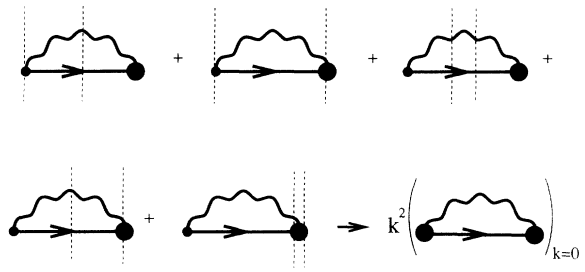

FIG. 8. Contributions to the leading k^2 dependence of the smectic self-energy. The vertical dashed lines indicate the extraction of a factor of k from the cut propagator or vertex. The net effect of the expansion is to dress both vertices in this one-loop contribution.

$$\Sigma_t(\mathbf{k})=\int \frac{d^3q}{(2\pi)^3}(-q_0 a\xi_\perp^2)^2|\hat{\mathbf{q}}_\perp\times(2\mathbf{k}_\perp+\mathbf{q}_\perp)|^2 \times D_t(\mathbf{q})G(\mathbf{k}+\mathbf{q}) \tag{25b}$$

and

$$\Pi_s(\mathbf{k})=\int \frac{d^3q}{(2\pi)^3}(-q_0 a\xi_\perp^2)^2[\hat{\mathbf{k}}_\perp\cdot(2\mathbf{q}_\perp+\mathbf{k}_\perp)]^2 \times G(\mathbf{q})G(\mathbf{k}+\mathbf{q}) , \tag{26a}$$

$$\Pi_t(\mathbf{k})=\int \frac{d^3q}{(2\pi)^3}(-q_0 a\xi_\perp^2)^2|\hat{\mathbf{k}}_\perp\times(2\mathbf{q}_\perp+\mathbf{k}_\perp)|^2 \times G(\mathbf{q})G(\mathbf{k}+\mathbf{q}) . \tag{26b}$$

[Note that these equations are only valid for the finite k dependence of the self-energies; Eqs. (9) and (10) are to be used when the external momentum is identically zero.] Terms with mixed splay and twist vertices yield zero upon integration.

The integrals in Eqs. (25) are evaluated after expanding G to fourth order in $\mathbf{k}$. The resulting form for the ψ self-energy is

$$\Sigma(\mathbf{k})=\Sigma(0)+\frac{aq_0^2\xi_\perp^2}{\pi\beta K_1\xi_\parallel}[f_\perp\xi_\perp^2k_\perp^2-f_\parallel\xi_{\parallel a}^2(k_\parallel-q_0)^2 -g_\perp\xi_\perp^4k_\perp^4] , \tag{27}$$

where $\xi_{\parallel a}\equiv\xi_\parallel a^{1/2}$. The explicit forms of $f_\perp$, $f_\parallel$, and $g_\perp$ were determined by integration and collection of terms (see Appendix):

$$f_\perp=\frac{5b_1-8}{16(1-b_1)^2}+\frac{(b_1-2)(b_1-4)}{16(1-b_1)^{5/2}}\tanh^{-1}\sqrt{1-b_1} +\frac{b_2}{b_1}\frac{1}{2(1-b_2)^{1/2}}\tanh^{-1}\sqrt{1-b_2} , \tag{28a}$$

$$f_\parallel=-\frac{3}{8(1-b_1)^2}+\frac{b_1(b_1+2)}{8(1-b_1)^{5/2}}\tanh^{-1}\sqrt{1-b_1} , \tag{28b}$$

$$g_\perp=-\frac{33b_1^2-98b_1+80}{256(1-b_1)^3} -\frac{b_1^3-24b_1^2+72b_1-64}{256(1-b_1)^{7/2}}\tanh^{-1}\sqrt{1-b_1} -\frac{b_2}{b_1}\frac{1}{16(1-b_2)}-\frac{3b_2-4}{16(1-b_2)^{5/2}}\tanh^{-1}\sqrt{1-b_2} , \tag{28c}$$

where $b_1=(K_3/\xi_\parallel^2)/(K_1/\xi_\perp^2)$ and $b_2=(K_3/\xi_\parallel^2)/(K_2/\xi_\perp^2)$. Comparison of Eqs. (6a), (14), and (27) yields expressions for the anisotropic correlation functions:

$$\xi_\perp^2=\frac{\xi_{\perp 0}^2}{a}-\frac{q_0^2\xi_\perp^4}{\pi\beta K_1\xi_\parallel}f_\perp , \tag{29a}$$

$$\xi_\parallel^2=\frac{\xi_{\parallel 0}^2}{a}+\frac{q_0^2\xi_\perp^2\xi_\parallel}{\pi\beta K_1}f_\parallel . \tag{29b}$$

Similarly, evaluation of Eqs. (26) yields

$$\Pi_{ss}(\mathbf{k})=\Pi_{ss}(0)-h_1K_{10}k_\perp^2-h_3K_{30}k_3^2 , \tag{30a}$$

$$\Pi_{tt}(\mathbf{k})=\Pi_{tt}(0)-h_2K_{20}k_\perp^2-h_3K_{30}k_3^2 , \tag{30b}$$

where

$$h_1=0 , \tag{31a}$$

$$h_2=\frac{q_0^2\xi_\perp^2}{24\pi\beta K_{20}\xi_\parallel} , \tag{31b}$$

$$h_3=\frac{q_0^2\xi_\parallel}{24\pi\beta K_{30}} . \tag{31c}$$

Thus, the splay elastic constant is not renormalized:

$$K_1=K_{10} . \tag{32}$$

The form of the corrections to K_2 and K_3 is similar to that found by de Gennes [7] and by Jähnig and Brochard [12], but the actual dependence on temperature is different due to the anisotropic divergences that we find for $\xi_\perp$ and $\xi_\parallel$:

$$K_2=K_{20}+\frac{q_0^2\xi_\perp^2}{24\pi\beta\xi_\parallel} , \tag{33}$$

$$K_3=K_{30}+\frac{q_0^2\xi_\parallel}{24\pi\beta} . \tag{34}$$

VII. NUMERICAL SOLUTION OF THE SCALED, COUPLED EQUATIONS

The growth of the correlation lengths and elastic constants can be found for arbitrary temperatures by solving the four coupled equations (29a), (29b), (33), and (34). The form of these equations can be simplified by making the following definitions:

$$a_{30}\equiv\left[\frac{q_0^2\xi_{\parallel 0}}{24\pi\beta K_{30}}\right]^2 , \tag{35a}$$

$$a' \equiv \frac{a}{a_{30}} , \tag{35b}$$

$$R \equiv \frac{(\xi_\perp/\xi_{\perp 0})^2}{(\xi_\parallel/\xi_{\parallel 0})^2} , \tag{35c}$$

$$L \equiv \frac{(\xi_\perp/\xi_{\perp 0})^2}{\xi_\parallel/\xi_{\parallel 0}} a_{30}^{1/2} , \tag{35d}$$

$$b_{10} \equiv \frac{K_{30}/\xi_{\parallel 0}^2}{K_1/\xi_{\perp 0}^2} , \tag{35e}$$

$$b_{20} \equiv \frac{K_{30}/\xi_{\parallel 0}^2}{K_{20}/\xi_{\perp 0}^2} . \tag{35f}$$

Then Eqs. (29) become

$$L^2 = \frac{R}{a'} - 24 b_{10} L^3 f_\perp , \tag{36a}$$

$$L^2 = \frac{R^2}{a'} + 24 b_{10} L^3 f_\parallel , \tag{36b}$$

where $f_\perp$ and $f_\parallel$ are functions of $b_1 = b_{10}(R+L)$ and $b_2 = b_{20}(R+L)/(1+b_{20}L)$. The two Eqs. (36) summarize our results; their solution depends only on three ratios: K_{30}/K_1, K_{30}/K_{20}, and $\xi_{\perp 0}/\xi_{\parallel 0}$.

In the high-temperature limit, where a' is large, we have the expected isotropic behavior of the correlation lengths, which means that $R=1$ and $L \propto \xi_\perp/\xi_{\perp 0} \propto 1/\sqrt{a'}$. In fact, by looking at Eqs. (36) we see that $L \to 1/\sqrt{a'}$ for large a' since $f_\perp$ and $f_\parallel$ (and their arguments b_1 and b_2) approach constants. In the low-temperature limit, $a' \to 0$, the self-consistent solution to Eqs. (36) and b_1 and b_2 yields b_1, b_2, $f_\perp$, $f_\parallel$, and L all approach constants, while $R \propto a'$. Specifically, as $a' \to 0$,

$$L \to \frac{1}{24 b_{10} f_\parallel} . \tag{37}$$

This behavior of L implies that $\xi_\parallel$ is diverging twice as rapidly as $\xi_\perp$ in the asymptotic region, i.e.,

$$\nu_\parallel = 2\nu_\perp . \tag{38}$$

This strong anisotropy is the same behavior as that found by Nelson and Toner close to but below the transition [4]. Looking at R we find that $R \propto (\xi_\parallel/\xi_{\parallel 0})^{-1} \propto a' \Longrightarrow \xi_\parallel/\xi_{\parallel 0} \propto 1/a' \Longrightarrow \nu_\parallel = \gamma$. Noting that $b_1 \to b_{10}L$, we can solve the asymptotic transcendental equation for b_1 [Eq. (37)] to find

$$b_1 \to 1.2190\ldots \tag{39}$$

and

$$L \to 1.2190\ldots/b_{10} . \tag{40}$$

Writing Eq. (33) in terms of our scaled quantities, we find

$$K_2 = K_{20}(1+b_{20}L) , \tag{41}$$

which means that K_2 approaches a constant as $a' \to 0$. So while K_2 begins to renormalize at higher reduced temperatures, asymptotically it does not diverge. In fact, the fractional increase in K_2 is $1+b_1(K_{10}/K_{20}) = 1+1.219(K_{10}/K_{20})$. Hence the increase in K_2 may not be much more than a factor of 3 for typical polar liquid-crystal systems.

Interesting and novel behavior occurs for intermediate values of a' where the correlation lengths and elastic constants cross over from high-temperature isotropic behavior to the low-temperature strongly anisotropic limit. The crossover is gradual and broad. The results of our model are weakly anisotropic at these intermediate temperatures. The specific behavior can be seen in Figs. 9–16, which result from numerical solutions to Eqs. (36). Figure 9 shows a log-log plot of $\xi_\perp/\xi_{\perp 0}$ and $\xi_\parallel/\xi_{\parallel 0}$ versus a' for $K_{30}/K_{10}=2$, $K_{30}/K_{20}=3$, and $\xi_{\parallel 0}/\xi_{\perp 0}=7$. These parameter values were chosen because they are typical of (polar) liquid-crystal systems [11]. For large a' the two correlation lengths diverge as predicted by an isotropic theory: $\xi/\xi_0 = 1/\sqrt{a'}$. At lower temperatures the growth rate of $\xi_\perp$ is reduced, as seen by the shallower slope. Finally, in the strongly anisotropic regime, we again have $\xi_\perp \propto 1/\sqrt{a'}$, but $\xi_\parallel \propto 1/a'$. For the set of parameters chosen we see that the intermediate, weakly anisotropic regime extends over about eight orders of magnitude in a'. (This would correspond to roughly six orders of magnitude in reduced temperature if $\gamma \approx 1.25$.)

The deviation from high-temperature (3D x-y) behavior is seen more clearly in Fig. 10, which is a plot of $\xi_{\perp,\parallel}/\xi_{xy}$. Figure 11 shows the effective correlation length exponents $\nu_{\perp,\parallel}/\gamma = d\ln\xi/d\ln a'$. $\nu_\perp/\gamma$ drops to ~ 0.4 in the middle of the weakly anisotropic region, yielding an anisotropy ratio of $\nu_\parallel/\nu_\perp = \frac{5}{4}$. If this intermediate region were sufficiently wide $\nu_\perp/\gamma$ would reach a minimum of $\frac{3}{8}$, which would give $\nu_\parallel/\nu_\perp = \frac{4}{3}$. For the parameters used in Figs. 9 and 10 the effect of the weakly anisotropic region is to reduce $\xi_\perp$ by an order of magnitude over what it would have been in the low-temperature regime had the $\delta\mathbf{n}$-ψ coupling not produced the weakly anisotropic region.

The qualitative features of the curves in Figs. 9–11 are dependent on the three ratios of initial parameters. In order to see the nature of these dependencies, we define four crossover temperatures, namely the temperatures at which $\xi_\perp$ and $\xi_\parallel$ change their rate of divergence, and the temperatures at which K_3 and K_2 begin to diverge.

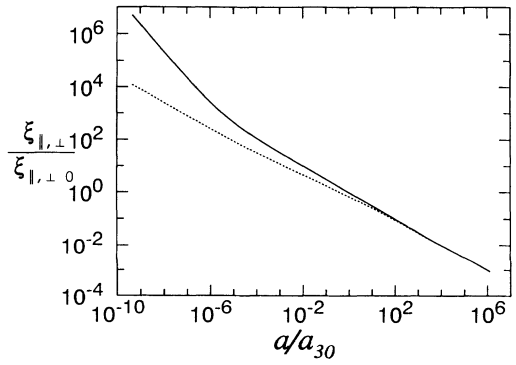

FIG. 9. Plot of the perpendicular (broken line) and parallel (solid line) correlation lengths for $\xi_{\parallel 0}/\xi_{\perp 0}=7$, $K_{30}/K_1=2$, and $K_{30}/K_{20}=3$.

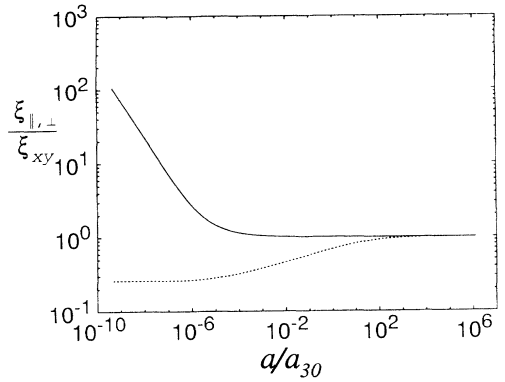

FIG. 10. Plot of $\xi_\perp/\xi_{xy}$ (broken line) and $\xi_\parallel/\xi_{xy}$ (solid line), showing the deviation of the critical behavior of these quantities from their 3D xy behavior, for $\xi_{\parallel 0}/\xi_{\perp 0}=7$, $K_{30}/K_1=2$, and $K_{30}/K_{20}=3$.

Specifically, we define the crossover temperatures to be the points at which the correction terms in Eqs. (29) and (31) are equal to the "bare" values. (In the case of $\xi_\perp^2$ it is the temperature at which the negative correction is half of ξ_{10}^2). We then find

$$a_\perp=\left[\frac{2q_0^2\xi_{10}^2}{\pi\beta K_1\xi_{\parallel 0}a_\parallel^{2\delta_\parallel}}f_\perp\right]^{2/(1-2\delta_\parallel)}, \tag{42a}$$

$$a_3=\left[\frac{q_0^2\xi_{\parallel 0}a_\parallel^{\delta_\parallel}}{24\pi\beta K_{30}}\right]^{2/(1+2\delta_\parallel)}, \tag{42b}$$

$$a_2=\left[\frac{q_0^2\xi_{10}^2}{24\pi\beta K_{20}\xi_{\parallel 0}a_\perp^{2\delta_\perp}a_\parallel^{\delta_\parallel}}\right]^{2/(1-4\delta_\perp-2\delta_\parallel)}, \tag{42c}$$

$$a_\parallel=\left[\frac{q_0^2\xi_{10}^2}{\pi\beta K_1\xi_{\parallel 0}a_\perp^{2\delta_\perp}}f_\parallel\right]^{2/(1-4\delta_\perp)}, \tag{42d}$$

where

$$-\delta_\perp\equiv\frac{\nu_\perp}{\gamma}-\tfrac{1}{2}, \tag{43a}$$

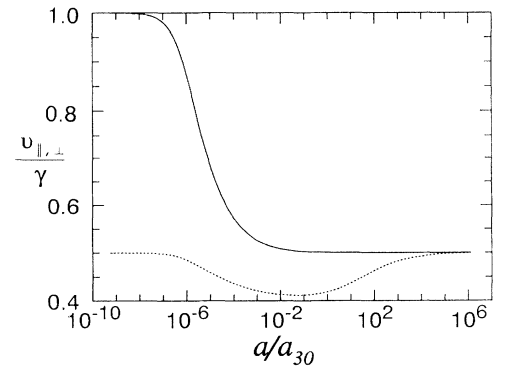

FIG. 11. Plot of the perpendicular (broken line) and parallel (solid line) effective correlation length exponents for $\xi_{\parallel 0}/\xi_{\perp 0}=7$, $K_{30}/K_1=2$, and $K_{30}/K_{20}=3$.

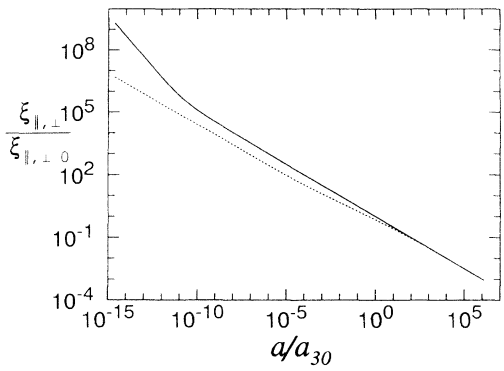

FIG. 12. Plot of the perpendicular (broken line) and parallel (solid line) correlation lengths for $\xi_{\parallel 0}/\xi_{\perp 0}=10$, $K_{30}/K_1=0.01$, and $K_{30}/K_{20}=10$.

$$\delta_\parallel\equiv\frac{\nu_\parallel}{\gamma}-\tfrac{1}{2}. \tag{43b}$$

For physically reasonable values of the "bare" parameters, the crossover temperatures are arranged so that $a_\parallel\approx a_2<a_\perp\approx a_3$. By comparing Eqs. (42a) and (42b) we find that $a_3>a_\perp$ if $48b_1f_\perp<1$. This is true for $b_{10}\approx b_{20}<\sim 0.008$. For the parameters used in Figs. 9–11 we have $b_{10}=2/7^2=0.04$ and $b_{20}=3/7^2=0.06$, so $a_\perp/a_{30}>a_3/a_{30}=1$. So $a_\perp$ and a_3 mark the high-temperature end of the weakly anisotropic region for physically realistic parameters.

The low-temperature end of the weakly anisotropic region is marked by a_2 and $a_\parallel$. Comparing Eqs. (42c) and (42d) shows that $a_2<a_\parallel$ if $f_\parallel\le K_1/24K_{20}$. In the low-temperature limit we have $f_\parallel\to 1/24b_{10}L\to 0.034$. The case we have shown in Figs. 9–11 has $K_1/24K_{20}=0.0625$, so a_2 is slightly larger than $a_\parallel$.

In order to understand the behavior of our theory more completely, it is instructive to consider several limiting cases in which the parameters vary from currently accessible experimental values. If splay were stiff enough compared to twist, a_2 might move up to the temperature region where $a_\perp$ is. Specifically, we would have $a_2\ge a_\perp$ if $f_\perp\le K_1/48K_{20}$. Figures 12 and 13 show the correlation

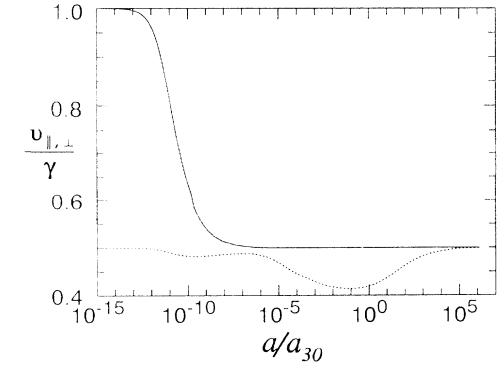

FIG. 13. Plot of the perpendicular (broken line) and parallel (solid line) effective correlation length exponents for $\xi_{\parallel 0}/\xi_{\perp 0}=10$, $K_{30}/K_1=0.01$, and $K_{30}/K_{20}=10$.

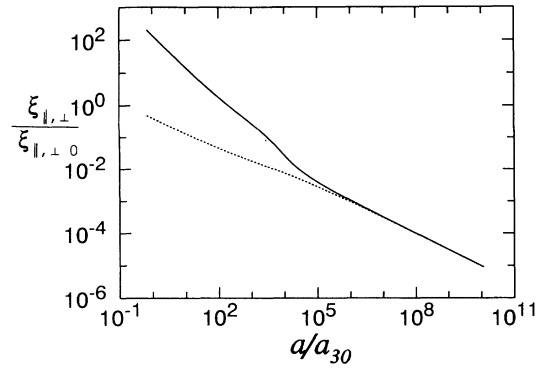

FIG. 14. Plot of the perpendicular (broken line) and parallel (solid line) correlation lengths for $\xi_{\parallel 0}/\xi_{\perp 0}=10$, $K_{30}/K_1=10^6$, and $K_{30}/K_{20}=0.01$.

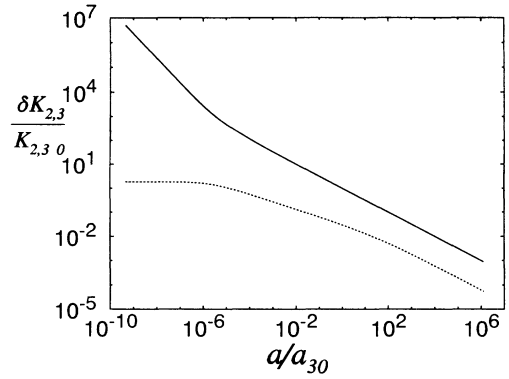

FIG. 16. Plot of the corrections to the twist (broken line) and bend (solid line) elastic constants for $\xi_{\parallel 0}/\xi_{\perp 0}=7$, $K_{30}/K_1=2$, and $K_{30}/K_{20}=3$.

lengths and critical exponents for the case where $\xi_{\parallel 0}/\xi_{\perp 0}=10$, $K_{30}/K_1=0.01$, and $K_{30}/K_{20}=10$. Here the renormalization of K_2 drives the onset of the weakly anisotropic region and decreases $\nu_\perp/\gamma$ from its isotropic value of 0.5. But as a is decreased $\nu_\perp/\gamma$ begins to recover before $a_\perp$ is reached, causing a second, less dramatic decrease in $\nu_\perp/\gamma$.

It is also possible theoretically to have $a_\parallel \geq a_\perp$. Comparing Eqs. (42a) and (42d) we find the condition for the onset of change in the renormalization of $\xi_\perp$ to occur at a higher temperature than the change in the renormalization of $\xi_\perp$ to be $f_\parallel \geq 2f_\perp$. If twist were sufficiently stiff to cause the last term in Eq. (28a) to be negligible, then this condition would be equivalent to $b_1=(K_3/\xi_{\parallel 0}^2)/(K_1/\xi_{\perp 0}^2)\geq 3.7$. Figures 14 and 15 show the correlation lengths and critical exponents for parameters that meet this condition. Note that once the critical behavior of $\xi_\perp$ changes, its rate of growth is quite dramatic until the $\delta\mathbf{n}$-ψ corrections to $\xi_\perp$ become important (below $a_\perp$), at which point the rate of growth of $\xi_\parallel$ drops again and then finally rises to the asymptotic rate with $\nu_\parallel/\gamma=1$. Regardless of the values of initial parameters and the order of the crossover temperatures, the asymptotic critical region in our model is strongly anisotropic, with $\nu_\parallel/\nu_\perp=2$.

Finally, the corrections to the twist and bend elastic constants for the physically realistic parameters are shown in Fig. 16. Because δK_2 depends on $\xi_\perp$, its behavior changes character at the same temperatures as $\xi_\perp$. The asymptotic constant value of δK_2 reflects the strong anisotropy $\nu_\parallel/\nu_\perp=2(\Longrightarrow \xi_\perp^2/\xi_\parallel \rightarrow$ constant). δK_3, which depends only on $\xi_\parallel$, does not change from the high-temperature behavior until the strongly anisotropic region is reached.

The results outlined above in the strongly anisotropic regime are what would be seen if the N-A transition were second order. Previous theoretical work [3] and experimental measurements [18] as well as preliminary calculations based on the model used in this paper indicate that the N-A transition may be weakly first order. The first-order transition may be encountered as the strongly anisotropic region is approached, making this region inaccessible except by supercooling the sample.

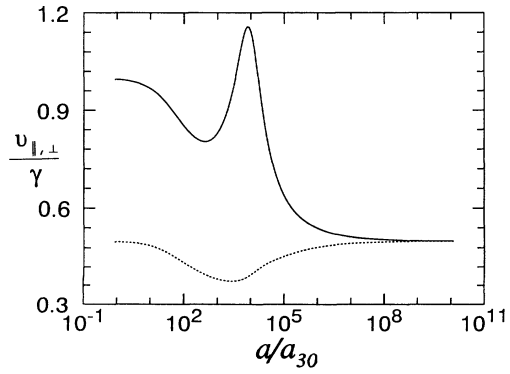

FIG. 15. Plot of the perpendicular (broken line) and parallel (solid line) effective correlation length exponents for $\xi_{\parallel 0}/\xi_{\perp 0}=10$, $K_{30}/K_1=10^6$, and $K_{30}/K_{20}=0.01$.

VIII. SELF-CONSISTENCY OF THEORY: CALCULATION OF CRITICAL EXPONENT $\eta_\perp$ AND $\eta_\parallel$

In this section we complete the calculation of the correlation function exponents, which provides a useful consistency check of our model. In particular, the correlation function critical exponents must satisfy the scaling relation $\nu=\gamma/(2-\eta)$. In order to check the self-consistency of this model we calculate $\eta_\perp$ and $\eta_\parallel$ explicitly. Since we consider here only director-smectic fluctuations this amounts to neglecting the small value of η in the 3D xy model.

We again evaluate Eqs. (25a) and (25b), but this time in the limit that $1 \ll \xi_{\perp,\parallel}\mathbf{k}_{\perp,\parallel}$. The values for $\eta_\perp$ and $\eta_\parallel$ are defined by

$$G^{-1}(a=0,\mathbf{k}_\perp,k_\parallel=0)\propto k_\perp^{2-\eta_\perp}\ , \tag{44a}$$

$$G^{-1}(a=0,\mathbf{k}_\perp=0,k_\parallel)\propto k_\parallel^{2-\eta_\parallel}\ . \tag{44b}$$

Consider first $\eta_\parallel$. The contribution to Σ from Eq. (25b) is zero, since $k_\perp=0$. Evaluation of Eq. (25a) yields

$$\lim_{a\to 0}\Sigma_s(\mathbf{k}=k_\parallel\hat{\mathbf{e}}_\parallel)$$
$$=\lim_{a\to 0}\frac{aq_0^2\xi_\perp^2}{\beta K_1\xi_\parallel}\int\frac{d^3p}{(2\pi)^3}\frac{p_\perp^2}{p_\perp^2+b_1p_\parallel^2}\frac{1}{1+p_\perp^2+(p_\parallel+s_\parallel)^2}$$
$$=-\frac{\xi_{10}^2q_0^2}{4\beta K_1}\frac{\sqrt{b_1}}{(1+\sqrt{b_1})^2}(k_\parallel-q_0)\ , \tag{45}$$

where $\mathbf{p}_\perp=\xi_\perp\mathbf{q}_\perp$, $p_\parallel=\xi_\parallel q_\parallel$, and $s_\parallel=\xi_\parallel(k_\parallel-q_0)$. Note that the leading k dependence in Σ comes from $s_\parallel=\xi_\parallel(k_\parallel-q_0)$, which cancels the $\xi_\parallel$ in the prefactor for the integral. This, coupled with the critical behavior: $\xi_\perp\propto a^{1/2}$ leaves only nondivergent and nonvanishing factors as $a\to 0$. For small $k_\parallel$ this linear contribution to $G^{-1}(\mathbf{k})$ dominates the $k_\parallel^2$ dependence in $(G^0)^{-1}$ and indicates that $\eta_\parallel=1$. Thus $\nu_\parallel$ and $\eta_\parallel$ satisfy the scaling relation $\nu_\parallel=\gamma/(2-\eta_\parallel)$, consistent with $\nu_\parallel=\gamma$ as found in Sec. VII.

In order to evaluate $\eta_\perp$ we examine $\Sigma(\mathbf{k}=\mathbf{k}_\perp)$:

$$\lim_{a\to 0}\Sigma_s(\mathbf{k}=\mathbf{k}_\perp)$$
$$=\lim_{a\to 0}\frac{aq_0^2\xi_\perp^2}{\beta K_1\xi_\parallel}\int\frac{d^3p}{(2\pi)^3}\frac{(p_\perp^2+2\mathbf{p}_\perp\cdot\mathbf{s}_\perp)^2}{p_\perp^2}\frac{1}{p_\perp^2+b_1p_\parallel^2}$$
$$\times\frac{1}{1+|p_\perp+s_\perp|^2+p_\parallel^2}\ , \tag{46}$$

where $\mathbf{s}_\perp=\xi_\perp\mathbf{k}_\perp$. Explicit evaluation shows the linear term in $\mathbf{k}_\perp$ vanishes by symmetry, although its prefactor would have a temperature dependence which would cause it to vanish as $a\to 0$ in any case. Therefore the leading $k_\perp$ dependence in (46) is $k_\perp^2$, indicating that $\eta_\perp=0$. Thus $\nu_\perp$ and $\eta_\perp$ satisfy the scaling relation $\nu_\perp=\gamma/(2-\eta_\perp)$, consistent with $\nu_\perp=\gamma/2$, as found earlier.

IX. SUMMARY

We have presented the results of a self-consistent, one-loop model calculation for the nematic–smectic-A phase transition based on de Gennes' free energy. In particular we have calculated, at all temperatures, the fluctuation-induced renormalization of the correlation lengths parallel and perpendicular to the director, as well as the renormalized twist and bend elastic constants. The anisotropic renormalization of the correlation lengths ($\nu_\perp\neq\nu_\parallel$) and elastic constants arises directly from the manifestly anisotropic nature of the coupling between the director fluctuations and the smectic order parameter. For physically realistic values of the bare elastic constants and correlation lengths, the renormalization of the bend elastic constant and the change in the divergence rate of the perpendicular correlation length become significant at higher temperatures and mark the high-temperature onset of the weakly anisotropic region. The lower end of this intermediate scaling region is marked by a change in the character of the divergence of the parallel correlation length. In the weakly anisotropic region $\nu_\perp/\gamma$ is reduced from its isotropic, 3D xy value of 0.5 (neglecting η_{xy}) to one that approaches $\frac{3}{8}$. Below the weakly anisotropic region $\nu_\perp/\gamma$ returns to its high-temperature value of 0.5, and $\nu_\parallel/\gamma$ becomes 1. The weakly anisotropic region is quite broad (6–8 decades in a, which corresponds to 4–6 decades in reduced temperature) and the crossover at the high-temperature end is subtle, which would explain the experimental observation of correlation lengths whose temperature dependence is characterizable by a single exponent. Several factors affect the location of the onset of strong anisotropy. Liquid-crystal systems with smaller layer spacings (larger q_0), with smaller intrinsic anisotropies (smaller $\xi_{\parallel 0}/\xi_{\perp 0}$), or with softer splay modes (smaller K_1) will have larger values of the crossover temperature into the strongly anisotropic region. If this lower-temperature end of the weakly anisotropic region can be accessed experimentally, the crossover from weak anisotropy to strong anisotropy should be readily detectable.

Coupled with the onset of strongly anisotropic behavior should be an intervening first-order transition to the smectic-A phase. The reduced temperature at which such a first-order transition would occur, and changes in the effective value of γ due to the coupling between the director and density-wave fluctuations, will be discussed in a separate work.

ACKNOWLEDGMENTS

We are grateful to T. Lubensky, S. Kumar, and C. Garland for helpful discussions.

APPENDIX

Calculation of the smectic self-energy as given by Eqs. (25) involves the evaluation of several integrals of the type

$$I_{m,n,j}=\frac{aq_0^2\xi_\perp^2}{\beta K_{1,2}\xi_\parallel}\int\frac{d^3p}{(2\pi)^3}\frac{1}{p_\perp^2+b_{1,2}p_\parallel^2}\frac{p_\perp^{2m}p_\parallel^{2n}}{(1+p^2)^{m+n+j}}\ , \tag{A1}$$

where $\mathbf{p}_\perp=\xi_\perp\mathbf{q}_\perp$, $p_\parallel=\xi_\parallel q_\parallel$, and $j=1$ or 2 for the contributions to $f_{\perp,\parallel}$ and $g_\perp$, respectively. The integrand is independent of ϕ. The Θ integral can be written in the form

$$\int_{-1}^{1}d\mu\frac{(1-\mu^2)^{2m}\mu^{4n}}{1+(b-1)\mu^2}\ , \tag{A2}$$

while the p integral becomes

$$\int_0^\infty dp\frac{p^{2m+2n}}{(1+p^2)^{m+n+j}}\ . \tag{A3}$$

The integrand is then expanded to fourth order in the perpendicular external momentum, and to second-order in the parallel external momentum, yielding the results given in Eqs. (28) and (31).

[1] W. L. McMillan, Phys. Rev. A **7**, 1419 (1973); J. Als-Nielsen, R. J. Birgeneau, M. Kaplan, J. D. Litster, and C. Safinya, Phys. Rev. Lett. **39**, 352 (1977); C. R. Safinya, R. J. Birgeneau, J. D. Litster, and M. E. Neubert, *ibid.* **47**, 668 (1981); R. J. Birgeneau, C. W. Garland, G. V. Kasting, and B. M. Ocko, Phys. Rev. A **24**, 2624 (1981); C. W. Garland, M. Meichle, B. M. Ocko, A. R. Kortan, C. R. Safinya, L. J. Yu, J. D. Litster, and R. J. Birgeneau, *ibid.* **27**, 3234 (1983); B. M. Ocko, R. J. Birgeneau, and J. D. Litster, Phys. Rev. Lett. **52**, 208 (1984); A. R. Kortan, H. von Kanel, R. J. Birgeneau, and J. D. Litster, J. Phys. (Paris) **45**, 529 (1984); K. W. Evans-Lutterodt, J. W. Chung, B. M. Ocko, R. J. Birgeneau, C. Chiang, and C. W. Garland, Phys. Rev. A **36**, 1387 (1987); Li Chen, J. D. Brock, J. Huang, and S. Kumar, Phys. Rev. Lett. **67**, 2037 (1991); W. G. Bouwman and W. H. de Jeu, *ibid.* **68**, 800 (1992); G. Nounesis, K. I. Blum, M. J. Young, C. W. Garland, and R. J. Birgeneau, Phys. Rev. E **47**, 1910 (1993); C. W. Garland, G. Nounesis, M. J. Young, and R. J. Birgeneau, *ibid.* **47**, 1918 (1993).

[2] B. I. Halperin and T. C. Lubensky, Solid State Commun. **14**, 997 (1974); T. C. Lubensky and Jing-Huei Chen, Phys. Rev. B **17**, 366 (1978); S. G. Dunn and T. C. Lubensky, J. Phys. (Paris) **42**, 1201 (1981); J. Toner, Phys. Rev. B **26**, 462 (1982); C. Dasgupta, Phys. Rev. A **27**, 1262 (1983); C. Dasgupta, Phys. Rev. Lett. **55**, 1771 (1985); C. Dasgupta, J. Phys. (Paris) **48**, 957 (1987).

[3] B. I. Halperin, T. C. Lubensky, and S.-K. Ma, Phys. Rev. Lett. **32**, 292 (1974).

[4] D. R. Nelson and J. Toner, Phys. Rev. B **24**, 363 (1981).

[5] T. C. Lubensky and A. J. McKane, J. Phys. Lett. (Paris) **43**, L-217 (1982).

[6] T. C. Lubensky, J. Chim. Phys. (Paris) **80**, 31 (1983), and other references therein.

[7] P. G. de Gennes, Solid State Commun. **10**, 753 (1972).

[8] P. G. de Gennes, Mol. Cryst. Liq. Cryst. **21**, 49 (1973).

[9] B. R. Patton and B. S. Andereck, Phys. Rev. Lett. **69**, 1556 (1992).

[10] F. C. Frank, Discuss. Faraday Soc. **58**, 1 (1958); T. C. Lubensky, J. Chim. Phys. (Paris) **80**, 31 (1983).

[11] P. G. de Gennes, *The Physics of Liquid Crystals* (Oxford University Press, Oxford, 1975).

[12] F. Jähnig and F. Brochard, J. Phys. (Paris) **35**, 301 (1974).

[13] B. S. Andereck and B. R. Patton, J. Phys. (Paris) **48**, 1241 (1987).

[14] A. A. Abrikosov, L. P. Gorkov, and I. Ye. Dzyaloshinskii, *Quantum Field Theoretical Methods in Statistical Physics* (Pergamon, Edinburgh, 1965).

[15] S. K. Ma, *Modern Theory of Critical Phenomena* (Benjamin, New York, 1976).

[16] G. Baym, Phys. Rev. **127**, 1391 (1962); G. Baym and G. Grinstein, Phys. Rev. D **15**, 2897 (1977).

[17] S. Coleman and E. Weinberg, Phys. Rev. D **7**, 1888 (1973). In their words: "The point of this analysis is *not* that the loop expansion is a good approximation scheme because (the loop expansion parameter) is a small parameter; indeed, (it) is equal to one . . . The point is, rather, since the loop expansion corresponds to expansion in a parameter that multiplies the *total* Lagrange density, it is unaffected by shifts of fields . . ., and by the redefinition of the division of the Lagrangian into free and interacting parts associated with such shifts. The n-loop approximation to the effective potential thus preserves what we have identified as the main advantage of the effective potential method; it enables us to survey all possible vacuum states at once, and to compute higher-order corrections before deciding which vacuum the theory finally picks."

[18] P. E. Cladis, W. van Saarloos, D. A. Huse, J. S. Patel, J. W. Goodby, and P. L. Finn, Phys. Rev. Lett. **62**, 1764 (1989); M. A. Anisimov, P. E. Cladis, E. E. Gorodetskii, D. A. Huse, V. E. Podneks, V. G. Taratuta, W. van Saarloos, and V. P. Voronov, Phys. Rev. A **41**, 6749 (1990).